Electronic Supplementary Material (ESI) for RSC Advances.
This journal is © The Royal Society of Chemistry 2023

Supplementary Material

Fluorescent dual-mode sensor for the determination of graphene oxide and catechin in environmental or food field

Esther Pinilla-Peñalver[a,b], Adrián Esteban-Arranz[c,d], Ana M. Contento[a], Ángel Ríos[a,*]

[a]Department of Analytical Chemistry and Food Technology, University of Castilla-La Mancha, Avenue Camilo José Cela, s/n, 13071 Ciudad Real, Spain.

[b]Regional Institute for Applied Chemistry Research, IRICA, Avenue Camilo José Cela, 1, 13071 Ciudad Real, Spain.

[c]Department of Chemical Engineering, University of Castilla La-Mancha, Avenue Camilo José Cela, 12, 13071, Ciudad Real, Spain.

[d]Department of Polymeric Nanomaterials and Biomaterials, Polymer Science and Technology Institute (CSIC), Juan de la Cierva 3, 28006, Madrid, Spain.

[*]Corresponding author:

Prof. Dr. Ángel Ríos.

Phone.: +34926295232

E-mail address: Angel.Rios@uclm.es

ORCID: http://orcid.org/0000-0003-1728-3097

E-mail addresses and ORCID codes:

Esther Pinilla-Peñalver: Esther.Pinilla@uclm.es; https://orcid.org/0000-0002-2804-3876

Adrián Esteban-Arranz: Adrian.Esteban@ictp.csic.es; https://orcid.org/0000-0003-4953-8066

Ana M. Contento: AnaMaria.Contento@uclm.es; https://orcid.org/0000-0002-4732-2782

Table of contents:

S1. EXPERIMENTAL SECTION

Reagents and materials

Instrumentation

Synthesis of graphene oxide materials

Quantification of catechin by capillary electrophoresis

S2. RESULTS AND DISCUSSION

Evaluation of catechin effect over riboflavin fluorescence

Interference study

S3. FIGURES AND TABLES

S1. EXPERIMENTAL SECTION

Reagents and materials

All aqueous solutions were prepared with analytical grade reagents and deionized water purified with a Milli-Q system (Millipore, Bedford, MA, USA) that achieves a resistivity of 18.2 MΩ cm at 25 °C. Riboflavin (≥ 98.0%), (+)-catechin hydrate (≥ 98.0%), 4-morpholineethanesulfonic acid hydrate (MES, ≥ 99.5%), sodium hydroxide (98.0%), nitric acid (70.0%, purified by redistillation, ≥ 99.9% trace metals basis), sulfuric acid (99.9% purity), sodium nitrate (99.9% trace metals basis), potassium permanganate (ACS reagent, ≥ 99.0%), graphite powder (< 20 μm, synthetic), and hydrogen peroxide (contains inhibitor, 30 wt. %

in H_2O, ACS reagent) were acquired from Sigma Aldrich (Madrid, Spain) and non-pyrogenic water was purchased from Scientific Laboratory Supplies (Nottingham, UK).

For interference study, folic acid (≥ 99.0%), *L*-lysine monohydrochloride (≥ 98.0%), *L*-cysteine (≥ 98.5%), *L*-alanine (≥ 98.0%), *L*-glutamic acid (≥ 99.0%), *D*-(+)-glucose anhydrous (≥ 99.5%), *D*-(−)-fructose (≥ 99.0%), *D*-(+)-saccharose (≥ 99.5%), *DL*-malic acid (≥ 99.0%), sodium chloride (≥ 99.5%), magnesium sulphate (≥ 99.5%), potassium carbonate (≥ 99.0%), mercuric chloride (≥ 99.5%), ammonium nitrate (≥ 99.0%) were also acquired from Sigma-Aldrich (Madrid, Spain). *L*-ascorbic acid (≥ 99.7%), citric acid anhydrous (≥ 99.5%), sodium phosphate dibasic (≥ 98.0%), hydrochloric acid (37%) and diethyl ether (≥ 99.5%) were purchased from PanReac (Barcelona, Spain). Paraquat dichloride (≥ 99.9%) and (−)-epicatechin (≥ 90.0%) were obtained from Fluka Chemie (Buchs, UK).

Instrumentation

Fluorescence spectra were acquired on a QuantaMaster40 spectrofluorometer from photon technology international (PTI) equipped with a 75 W continuous xenon short-arc lamp using a detector voltage of 981 V. SOC-10 USB interface FelixGX software was used to collect and process fluorescence data. Emission and excitation slit widths were both 2 nm unless otherwise specified and a 3 mm quartz cuvette was used. For the determination of the luminescence lifetime of the species, the fluorescence decay was also measured on a PTI Time Master fluorimeter equipped with a picosecond nitrogen laser and a wavelength selector. This system was used with the dye 2-[1,1′-biphenyl]-4-yl-5-[4-(1,1′-dimethylethyl)phenyl]-1,3,4-oxadiazole (BPBD). The stroboscopic detector was coupled to a Czerny−Turner monochromator on the emission port. The system was connected to a personal computer via an ethernet interface and governed by Felix32. The instrumental parameters used were as follows: λ_{exc} = 368 nm and λ_{em} = 524 nm, 300 channels, integration time = 50 μs, 10 averages per decay, 5 shots

per channel, laser pulse frequency = 5 Hz, 5 nm excitation and emission slit widths, and a logarithmic collection step.

Absorption spectra were recorded in a UV-Vis spectrophotometer (SECOMAM UVI Light XS 2), equipped with a LabPower (V3-50) for absorbance data acquisition, along the 200 − 800 cm^{-1} spectral range. A 10 mm quartz cuvette was used for absorbance experiments. All measurements were performed at room temperature.

X-ray diffraction (XRD) experiments were performed in a Philips X'Pert MPD diffractometer at 40 mA and 40 kV with Cu Kα1 (1.54056 Å) radiation. A zero-background sample holder was used to deposit freeze-dried GO materials to make sure there was not any interference from the background. Raman spectra were acquired from 1000 to 2000 cm^{-1} by a Renishaw, InVia spectrometer. A 532 nm 1% power laser was used with a 50x magnification. 15 measurements per sample were recorded and their standard deviation values were calculated and incorporated into the results. OriginPro 8.5 software was used to normalize spectra by the intensity of the graphitic band (G). Scanning transmission electron microscopy (STEM) experiments were carried out to define materials morphology and lateral dimensions. A GeminiSEM 500 from the ZEISS brand was used in the STEM mode. Fourier-transform infrared spectroscopy (FT-IR) was used to elucidate GO surface chemistry. FT-IR experiments were performed on a Shimadzu IR instrument, IR-Affinity-1S model with a DTGS Standard detector. Samples were placed in an attenuated total reflectance (ATR) crystal of ZnSe and the measurements were acquired from 4000 to 450 cm^{-1}, with a 4 cm^{-1} resolution and 45 scans per sample. Results were repeated three times.

The pH of all aqueous solutions was measured using a Basic 20 pH-meter combined with a combined glass electrode (Crison Instruments S. A., Barcelona, Spain). An ultrasound bath (J. P. Selecta, Barcelona, Spain), a microcentrifuge Minicen (Ortoalresa S. A., Madrid, Spain), a freeze dryer LyoQuest (Telstar, Barcelona, Spain) and a vortex stirrer V05 series (LBX instruments, Madrid, Spain) with speed control were also used.

Synthesis of graphene oxide materials

In this work, three graphene oxide-based materials with control lateral dimensions and thicknesses were synthesized. Large graphene oxide (lGO) was produced following an experimental procedure described elsewhere.[1] In this case, the synthesis protocol followed a modified Hummers methodology. After the oxidation procedure, larger graphene oxide flakes were concentrated to the top of the graphitic residue by centrifugation and then removed by their solubilization with warm water. Next day, two rounds of purification steps were carried out by centrifugation. Additionally, small graphene oxide (sGO) flakes were produced after the sonication of lGO for 5 min and a posterior purification step by centrifugation. This methodology was reported by F. Rodrigues et al.[2] This study demonstrated the possibility to obtain smaller graphene oxide flakes with similar physicochemical characteristics as lGO only differing in their lateral dimensions. Finally, monolayer graphene oxide (mlGO) flakes were collected from the washing fraction prior the concentration of lGO.[3] The concentrations obtained for each of the GOs were 2.83, 2.50 and 0.45 mg mL^{-1} of lGO, sGO and mlGO, respectively. After their synthesis, GO solutions were frozen by liquid nitrogen at -77 K and sublimated at 0.005 mbar for 3 days.

Quantification of catechin by capillary electrophoresis

A previously validated electrophoretic procedure was used as a comparative analysis method for catechin quantification.The conditions of the capillary electrophoresis (CE) procedure were previously evaluated to achieve the best separation efficiency for the desired analyte since the cocoa matrix is complex and contains interferents. The electrophoretic separation was carried out in the positive polarity mode applying a voltage of 10 kV at 25 ºC. Standards and samples were injected by hydrodynamic injection mode for 15 s at 40 mbar. Detection was recorded at 278 nm. Aqueous buffer solution used for the separation of catechin

from the other compounds consisted of 50 mM anhydrous sodium tetraborate at pH 9.5.

S2. RESULTS AND DISCUSSION

Evaluation of catechin effect over riboflavin fluorescence

The effect of catechin on the fluorescence signal of riboflavin in the absence of GO was also evaluated. Control experiments were performed to verify that the return of the emission intensity was produced by the release of riboflavin from the complex by catechin, instead of by interactions between catechin and riboflavin. As expected, there was no spectroscopic overlap between catechin and riboflavin signals which indicates that there was no signal additivity after exciting at 445 nm (**Fig. S4A**). Moreover, the addition of increasing concentrations of catechin from 4.2 to 62.5 μg mL^{-1} to 1 μM riboflavin solution did not modify the initial fluorescence signal of the dye, as observed in **Fig. S4B**. This fact demonstrates that there was no interaction between both species.

Interference study

To assess the validity and test the selectivity of both GO and catechin sensors, several potential interfering substances were added into de sensing systems in the presence of the analyte under the optimal conditions. On the one hand, **Fig. S8A** displays the interference study to detect GO by monitoring the riboflavin fluorescence response in the presence of the nanomaterial with other commonly coexisting compounds. The concentration of all substances tested was 3-folds of lGO while that of paraquat was the same, specifically 15 μg mL^{-1}. Results revealed that no evident changes in the fluorescence intensity ratio I_0/I of the probing system were produced in the presence of other compounds tested, including $HgCl_2$, NH_4NO_3, Na_2HPO_4 and K_2CO_3. Meanwhile, paraquat as an herbicide probably present in environmental samples, would interfere in the detection of GO by ca. 10%. Therefore, a sample treatment should be performed,

or a separation technique should be used when the proposed method is applied. In conclusion, the obtained results suggest that the proposed strategy for the determination of GO shows good selectivity.

On the other hand, the selectivity of riboflavin-lGO probe towards catechin in relation to other coexisting species in food products was also evaluated. **Fig. S8B** shows the specificity of the established sensing system to other substances at a catechin concentration 10 μg mL^{-1}. As it can be observed, the enhanced fluorescence signal (I/I_0) of the probing system was unaffected at 5-fold concentration of the amino acids checked (a representative example of each of them according to their R-side chain: i) R-side chain with additional amino group (*L*-lysine), ii) thiol group (*L*-cysteine), iii) additional carboxylic functional group (*L*-glutamic acid) and iv) carbon chain either aromatic or aliphatic (*L*-alanine)), food additives (citric acid and malic acid) and salts (NaCl and $MgSO_4$) and 3-fold concentration of the typical sweeteners (glucose, fructose and sucrose). As it is common in food samples, some vitamins (ascorbic acid and folic acid) were tested as possible interferents at the same concentration level as catechin. Results revealed that while the presence of ascorbic acid (vitamin C) did not produce any change in the analytical signal, folic acid (vitamin B_9) showed interferences of ca. 22%. However, this enhanced of the analytical signal by the presence of folic acid is due to additivity between the fluorescent signals since this compound presents an emission band in the wavelength range studied.

Otherwise, catechin molecule presents two chiral centers in its structure: one is on carbon 2 and the other on 3. Therefore, catechin has four diastereomers. Two are isomers of the *trans*-configuration that are called catechin and the other two are of the *cis*-configuration that are called epicatechin. As an example, the addition of the most common isomer of epicatechin, (−)-epicatechin, was evaluated. After all, this is an enantiomer of (+)-catechin and, as expected, it produces a significant increase of about 36% over the analytical signal of the control. Therefore, these 4 species could be simultaneous detected, in fact many compounds present mixtures of enantiomers and the proportion of each of them is

not well-known. In view of these results, riboflavin-lGO system suggested to be selective for catechin determination even in coexistence with high concentrations of the tested substances.

References

1 D. A. Jasim, N. Lozano, K. Kostarelos. Synthesis of few-layered, high-purity graphene oxide sheets from different graphite sources for biology. *2D Mater*., 2016, **3**(1), 14006-14022. https://doi.org/10.1088/2053-1583/3/1/014006.

2 A. F. Rodrigues, L. Newman, N. Lozano, S. P. Mukherjee, B. Fadeel, C. Bussy, K. Kostarelos. A blueprint for the synthesis and characterisation of thin graphene oxide with controlled lateral dimensions for biomedicine. *2D Mater.,* 2018, **5**(3), 35020-35038. https://doi.org/10.1088/2053-1583/aac05c.

3 A. Esteban-Arranz, M. Á. Arranz, M. Morales, R. Martín-Folgar, J. Álvarez-Rodríguez. Thickness of graphene oxide-based materials as a control parameter. 2021.

S3. FIGURES AND TABLES

Fig. S1 (A) XRD diffractograms, (B) Raman profiles, (C) STEM micrographs, (D) FT-IR results, (E) UV-Vis and (F) fluorescence spectra of lGO, sGO and mlGO structures.

Fig. S2 Absorption (grey line) and fluorescence (blue line, dotted for excitation and solid for emission) spectra of riboflavin aqueous solution.

Fig. S3 Adsorption capability of lGO for riboflavin in the presence of different catechin concentrations between 1.1 and 108.3 μg mL^{-1}.

Fig. S4 (A) Emission profiles of riboflavin and catechin. The concentration of riboflavin was 0.38 μg mL^{-1} and the catechin was 62.5 μg mL^{-1}, λ_{exc} 445 nm and λ_{em} 524 nm. (B) Effect of catechin concentration on the fluorescence of riboflavin. The concentration of riboflavin was 0.38 μg mL^{-1}, 15 mmol L^{-1} MES, pH 6.5, 3 min interaction time, λ_{exc} 445 nm and λ_{em} 524 nm. Inset is represented the I/I_0 ratio against different concentration of catechin.

Fig. S5 (A – C) Optimization of the experimental variables for the detection of GO (exciting at 368 nm) and (D – F) catechin (exciting at 445 nm). (A) Influence of pH, (B) buffer concentration, (C) indicator concentration in the formation of riboflavin-lGO complex, expressed as riboflavin fluorescence extinction efficiency (I_0/I) and (D) quenching capacity of the different GO structures. (E) Effect of pH and (F) buffer concentration in the formation of riboflavin-lGO-catechin complex, expressed as riboflavin fluorescence recovery (I/I_0). Error bars are given to check the reproducibility (n = 5).

Fig. S6 Kinetic study of the interaction between riboflavin and (A) lGO, (B) sGO and (C) mlGO to form the corresponding complex. The concentration of riboflavin was 0.38 μg mL^{-1}, 18 μg mL^{-1} of lGO, 18 μg mL^{-1} of sGO, 16 μg mL^{-1} of mlGO, 15 mmol L^{-1} MES, pH 7.5, λ_{exc} 368 nm and λ_{em} 524 nm.

Fig. S7 Kinetic study of the interaction between catechin and riboflavin-lGO complex. The concentration of riboflavin was 0.38 μg mL^{-1}, 126.1 μg mL^{-1} of lGO, 8 and 35 μg mL^{-1} of catechin (circles and triangles, respectively), 15 mmol L^{-1} MES, pH 6.5, λ_{exc} 445 nm and λ_{em} 524 nm.

Fig. S8 (A) Selectivity of the stablished probing system to lGO (control) and lGO with other coexistence substances present in environmental matrices. The concentration of lGO was 15 μg mL^{-1} and the solutions were prepared in MES buffer at pH 7.5. (B) Fluorescence response of the riboflavin-GO system to catechin (control) and catechin in the presence of potential interfering compounds from food products. The concentration of catechin was 10 μg mL^{-1}. The solutions were prepared in MES buffer at pH 6.5.

Fig. S9 Analyses of (A) river water, (B) drinking water, (C) seawater (D) and soil samples fortified at different concentration levels of lGO between 1.1 and 4.0 μg mL^{-1}. The concentration of riboflavin was 0.38 μg mL^{-1}, 15 mmol L^{-1} MES, pH 7.5, 3 min interaction time, λ_{exc} 368 nm and λ_{em} 524 nm.

Fig. S10 Detection of catechin in (A) red wine and (B) green tea matrices doped with different concentrations from 10.0 and 36.6 μg mL^{-1}. The concentration on

riboflavin was 0.38 μg mL^{-1}, 126 μg mL^{-1} lGO, 15 mmol L^{-1} MES, pH 6.5, 1 min interaction time, λ_{exc} 445 nm and λ_{em} 524 nm.

Table S1. Raman results found for free GO and modified with riboflavin.

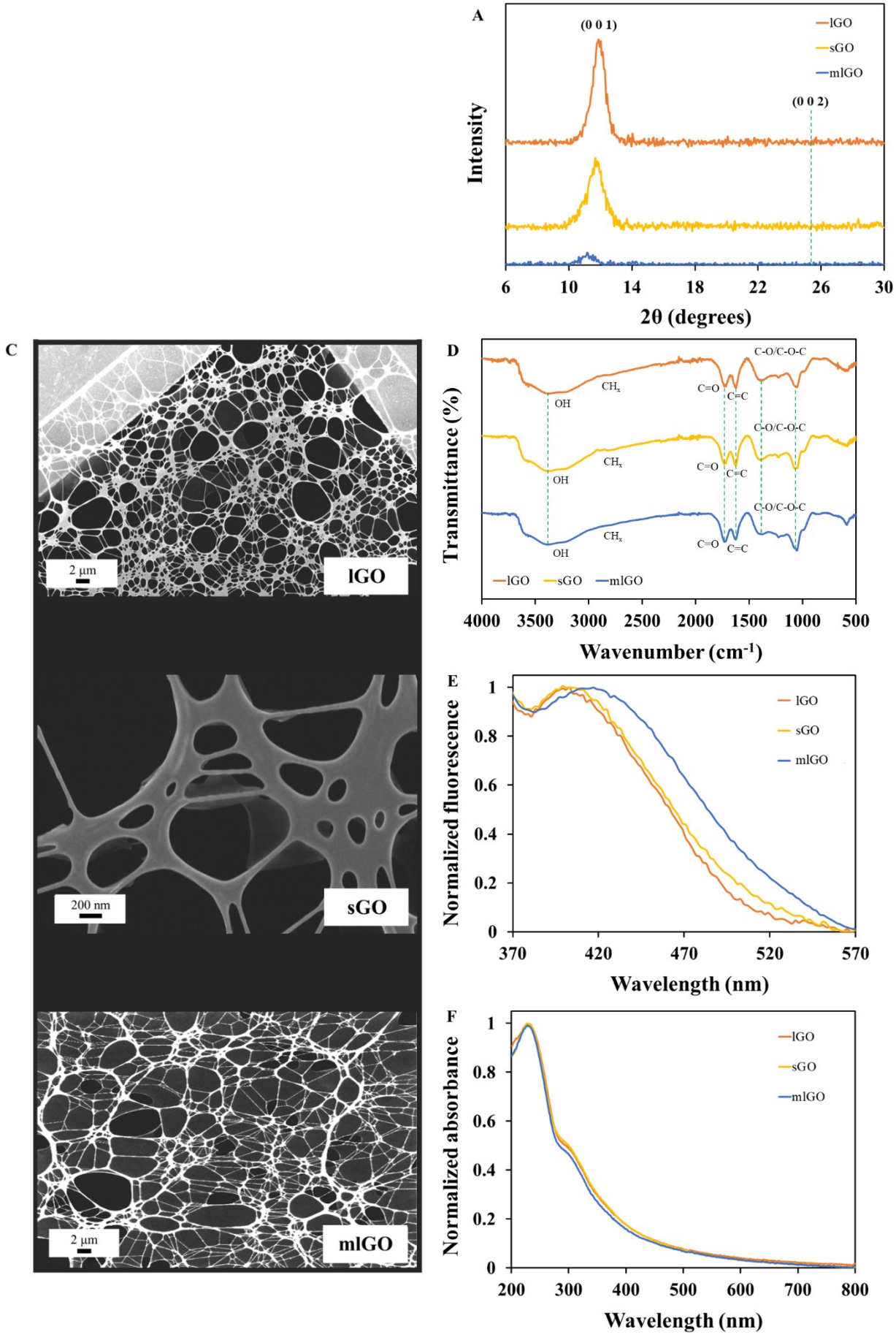
A
(0 0 1)
(0 0 2)
lGO
sGO
mlGO
Intensity
6
10
14
18
22
26
30
2θ (degrees)
C
2 μm
lGO
200 nm
sGO
2 μm
mlGO
D
Transmittance (%)
OH
CHx
C=O
C=C
C-O/C-O-C
lGO
sGO
mlGO
4000
3500
3000
2500
2000
1500
1000
500
Wavenumber (cm-1)
E
Normalized fluorescence
0
0.2
0.4
0.6
0.8
1
370
420
470
520
570
Wavelength (nm)
F
Normalized absorbance
200
300
400
500
600
700
800
Wavelength (nm)

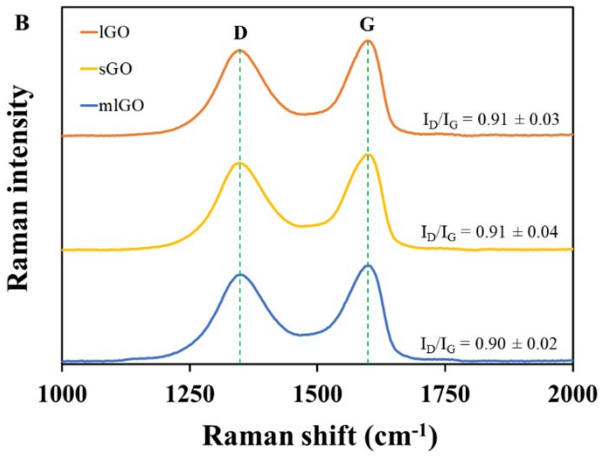
B
lGO
sGO
mlGO
D
G
I_D/I_G = 0.91 ± 0.03
I_D/I_G = 0.91 ± 0.04
I_D/I_G = 0.90 ± 0.02
Raman intensity
1000
1250
1500
1750
2000
Raman shift (cm^{-1})

Fig. S1

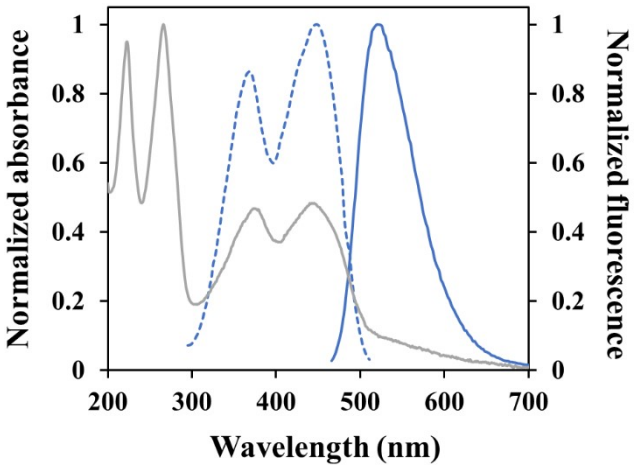
Normalized absorbance
Normalized fluorescence
0
0.2
0.4
0.6
0.8
1
200
300
400
500
600
700
Wavelength (nm)

Fig. S2

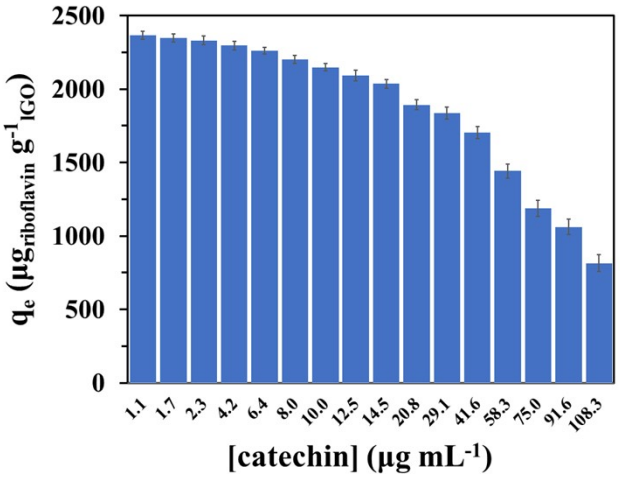
2500
2000
1500
1000
500
0
q_e ($\mu g_{riboflavin}$ g^{-1}_{IGO})
1.1
1.7
2.3
4.2
6.4
8.0
10.0
12.5
14.5
20.8
29.1
41.6
58.3
75.0
91.6
108.3
[catechin] (μg mL^{-1})

Fig. S3

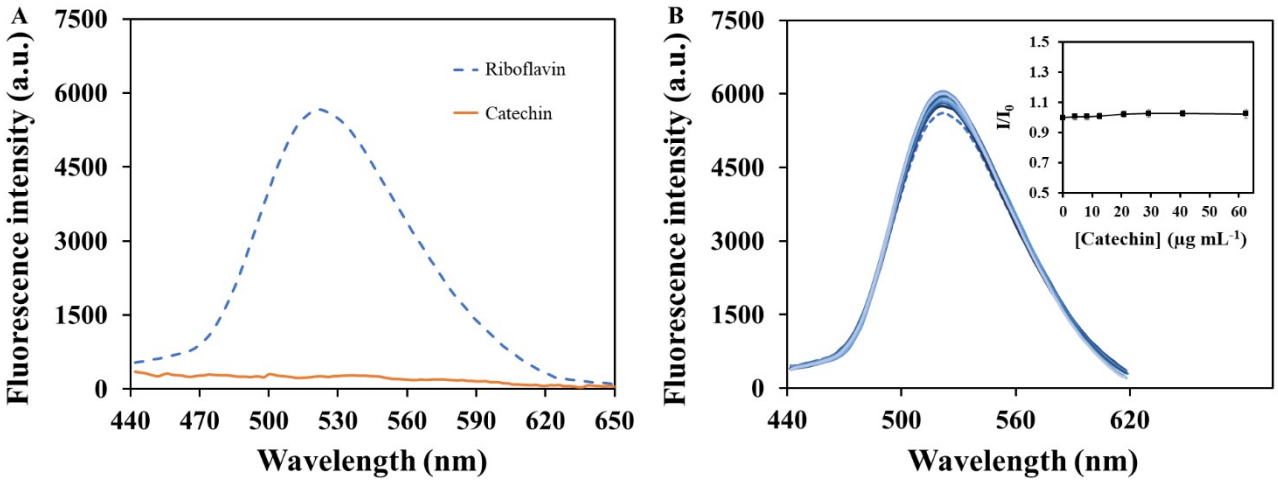
A
Fluorescence intensity (a.u.)
7500
6000
4500
3000
1500
0
Riboflavin
Catechin
440
470
500
530
560
590
620
650
Wavelength (nm)
B
Fluorescence intensity (a.u.)
7500
6000
4500
3000
1500
0
440
500
560
620
Wavelength (nm)
I/I0
1.5
1.3
1.1
0.9
0.7
0.5
0
10
20
30
40
50
60
[Catechin] (μg mL-1)

Fig. S4

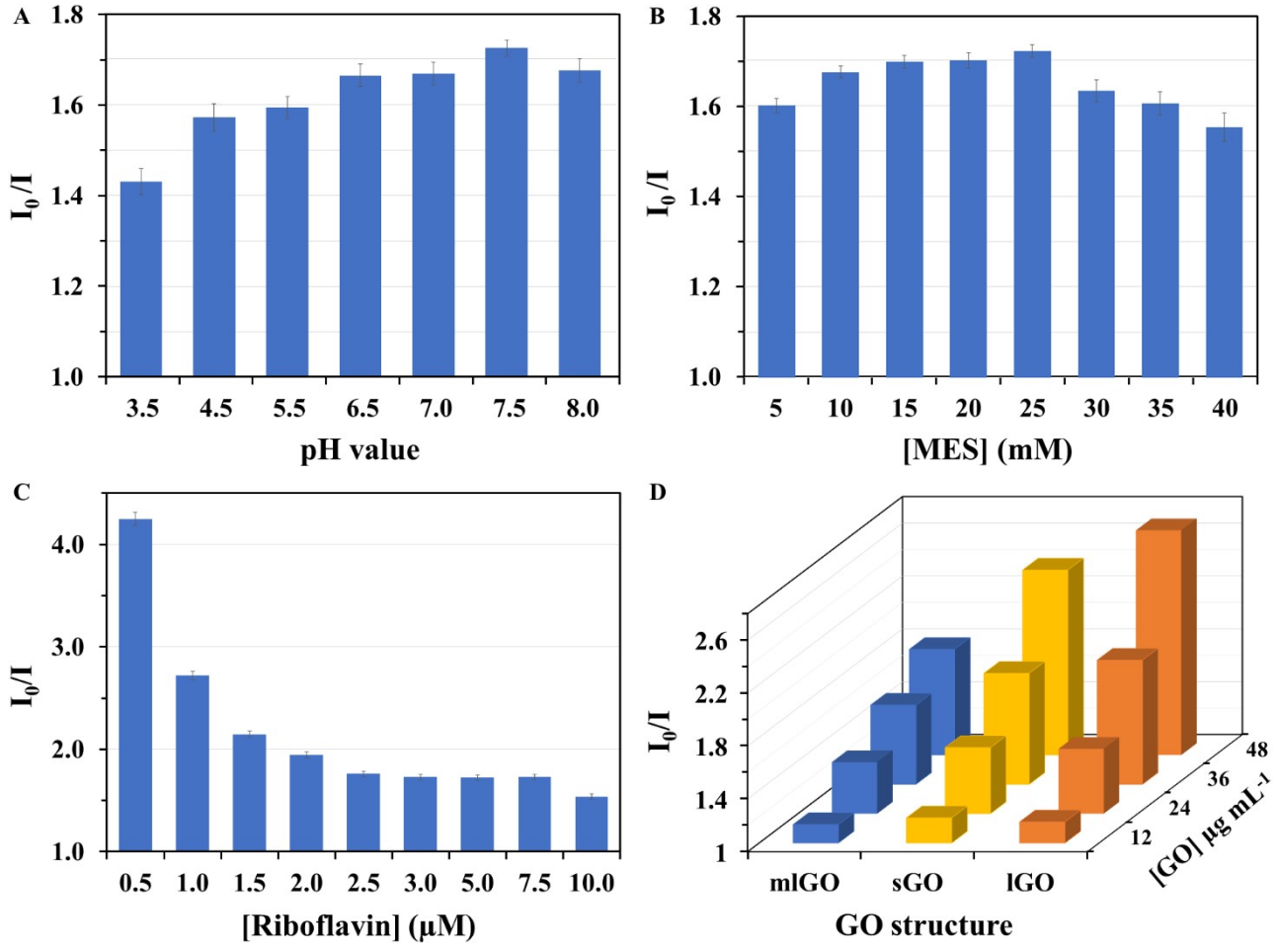
A
1.8
1.6
1.4
1.2
1.0
I0/I
3.5
4.5
5.5
6.5
7.0
7.5
8.0
pH value
B
1.8
1.6
1.4
1.2
1.0
I0/I
5
10
15
20
25
30
35
40
[MES] (mM)
C
4.0
3.0
2.0
1.0
I0/I
0.5
1.0
1.5
2.0
2.5
3.0
5.0
7.5
10.0
[Riboflavin] (μM)
D
2.6
2.2
1.8
1.4
1
I0/I
mlGO
sGO
lGO
GO structure
12
24
36
48
[GO] μg mL-1

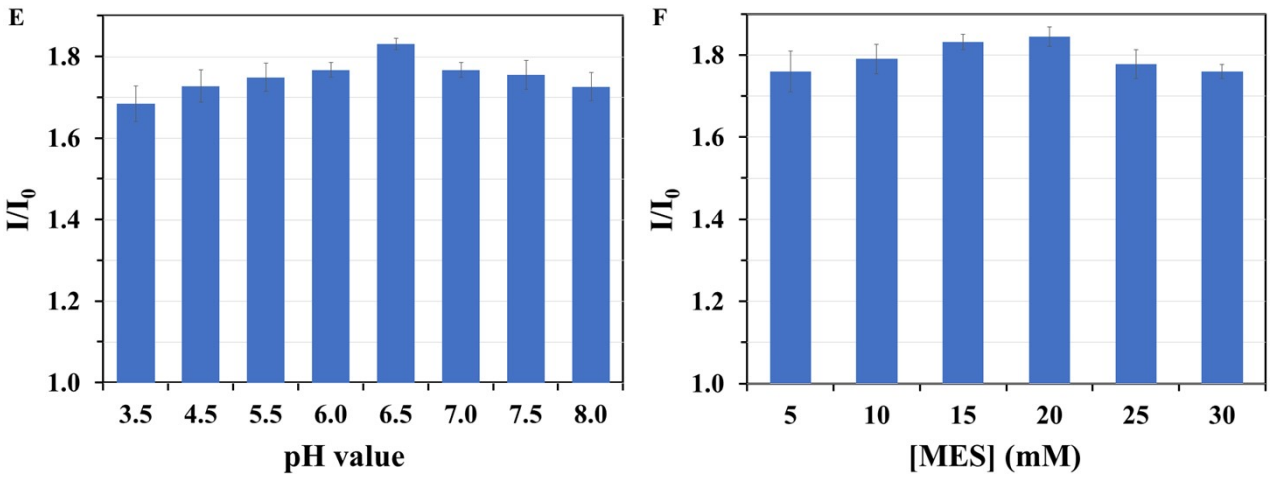
E
1.8
1.6
1.4
1.2
1.0
I/I0
3.5
4.5
5.5
6.0
6.5
7.0
7.5
8.0
pH value
F
1.8
1.6
1.4
1.2
1.0
I/I0
5
10
15
20
25
30
[MES] (mM)

Fig. S5

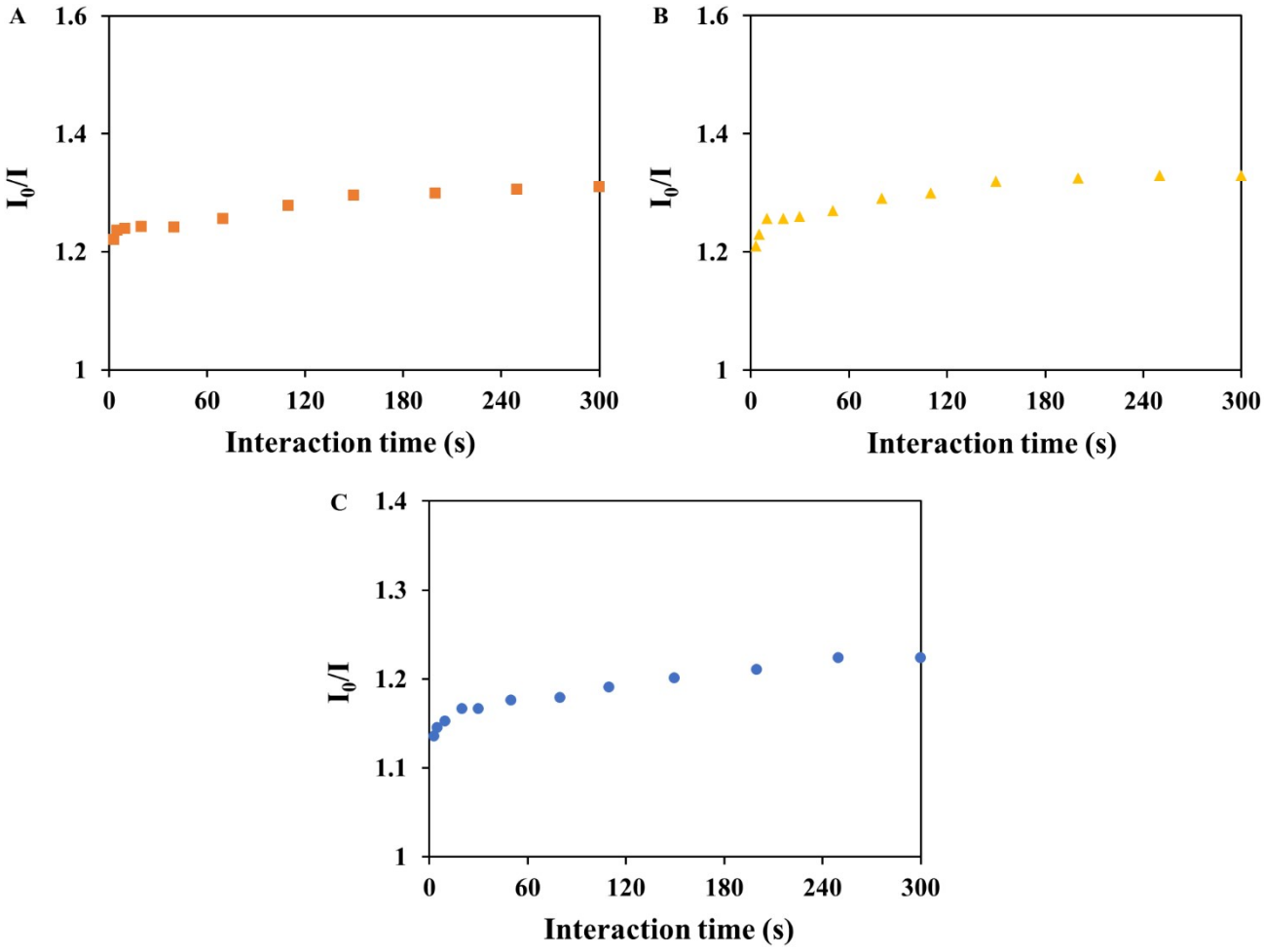
A
1.6
1.4
1.2
1
I0/I
0
60
120
180
240
300
Interaction time (s)
B
1.6
1.4
1.2
1
I0/I
0
60
120
180
240
300
Interaction time (s)
C
1.4
1.3
1.2
1.1
1
I0/I
0
60
120
180
240
300
Interaction time (s)

Fig. S6

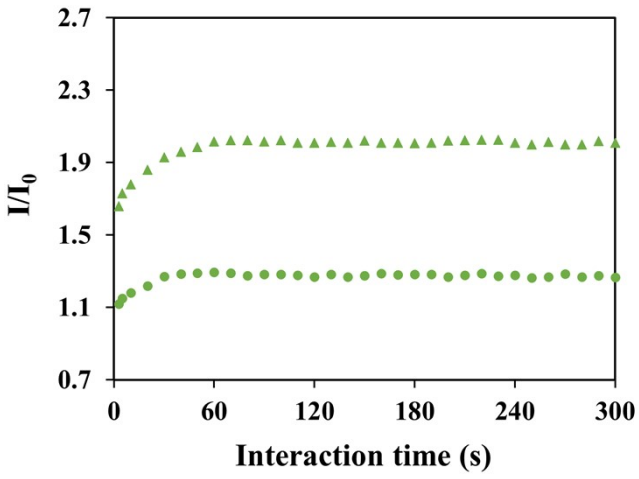

Fig. S7

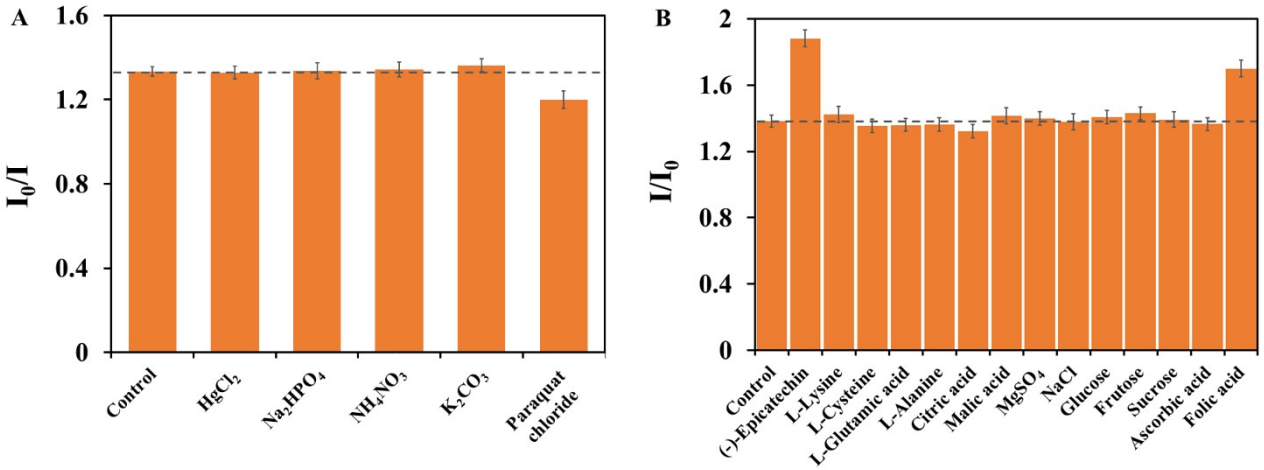
A
1.6
1.2
0.8
0.4
0
I_0/I
Control
$HgCl_2$
Na_2HPO_4
NH_4NO_3
K_2CO_3
Paraquat chloride
B
2
1.6
1.2
0.8
0.4
0
I/I_0
Control
(-)-Epicatechin
L-Lysine
L-Cysteine
L-Glutamic acid
L-Alanine
Citric acid
Malic acid
$MgSO_4$
NaCl
Glucose
Frutose
Sucrose
Ascorbic acid
Folic acid

Fig. S8

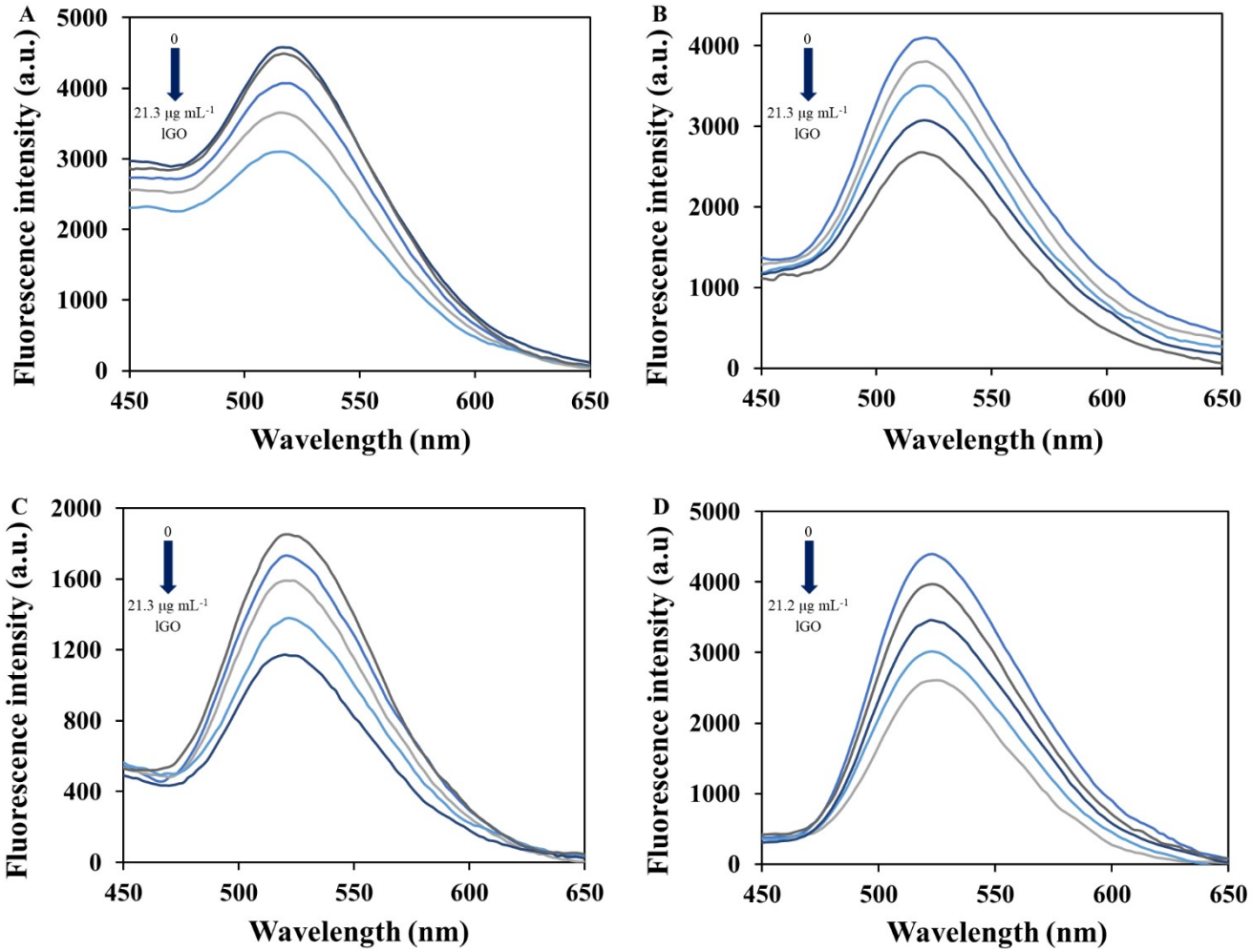
A
B
C
D
Fluorescence intensity (a.u.)
Wavelength (nm)
0
21.3 µg mL-1
lGO
21.2 µg mL-1
lGO

Fig. S9

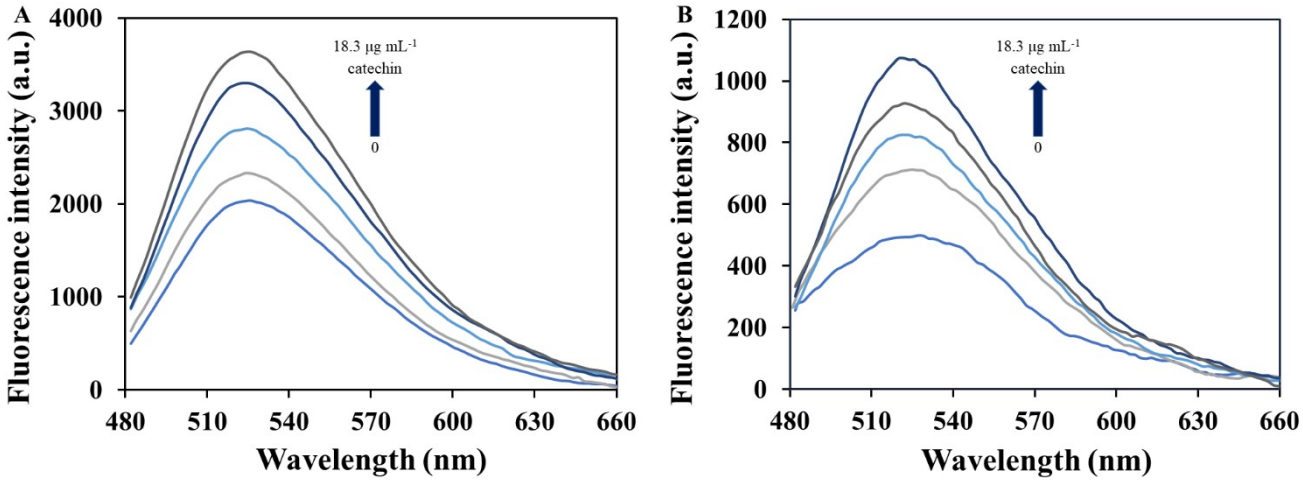
A
Fluorescence intensity (a.u.)
4000
3000
2000
1000
0
18.3 μg mL-1
catechin
0
480
510
540
570
600
630
660
Wavelength (nm)
B
Fluorescence intensity (a.u.)
1200
1000
800
600
400
200
0
18.3 μg mL-1
catechin
0
480
510
540
570
600
630
660
Wavelength (nm)

Fig. S10

Table S1.

Sample	I_D/I_G	Raman shift (cm^{-1})
		G band
lGO	0.91	1598.0
Riboflavin-lGO (1)	0.95	1589.6
Riboflavin-lGO (2)	0.95	1592.4
Riboflavin-lGO (3)	0.98	1596.2